Clays and Clay Minerals, Vol. 65, No. 1, 42–51, 2017.

CONTROLLABLE PREPARATION OF ZEOLITE P1 FROM METAKAOLIN-BASED GEOPOLYMERS *VIA* A HYDROTHERMAL METHOD

YUANHUI WANG[1], JIEYU CHEN[1,2,*], HONGDAN WU[3], AND XINRONG LEI[1]

[1]Faculty of Materials Science and Chemistry, China University of Geosciences, Wuhan 430074, PR China
[2]Engineering Research Center of Nano-Geo Materials of Ministry of Education, China University of Geosciences, Wuhan 430074, PR China
[3]College of Resources and Environmental Engineering, Wuhan University of Science and Technology, Wuhan 430081, PR China

Abstract—A more controllable method to synthesize particular zeolites from geopolymers is needed in order to effectively use these materials in industrial applications. In the present study, a well-crystallized zeolite P1 was synthesized from a metakaolin-based geopolymer (SiO_2/Al_2O_3=3.2) using a hydrothermal method. The products obtained by hydrothermal treatment were identified using X-ray diffraction (XRD), scanning electron microscopy (SEM), and specific surface areas. The XRD patterns and SEM micrographs indicated that the structure and morphology of zeolite P1 could be controlled by the NaOH solution concentration, hydrothermal temperature, and the hydrothermal treatment time. The crystalline structure of the prepared zeolite P1 was refined using the Rietveld method and the crystal structure parameters were as follows: a = 10.01 Å, b = 10.01 Å and c = 10.03 Å. The optimal hydrothermal conditions to form zeolite P1 were 24 h at a hydrothermal temperature of 100ºC and 2.0 M NaOH solution. Moreover, the synthesized zeolite P1 had a specific surface area of 36.56 m^2/g.

Key Words—Hydrothermal Method, Metakaolin-based Geopolymer, Zeolite P1.

INTRODUCTION

The name geopolymer was proposed by Davidovits (1991) for a material with a three dimensional network structure that is composed of silicon oxide tetrahedra and aluminum oxide tetrahedra. Provis and van Deventer (2009) described geopolymers as solid aluminosilicate materials usually prepared by using alkali hydroxides or alkali silicates to activate solid materials, such as coal fly ash, calcined clay, or metallurgical slag, and are primarily used as a low-CO_2 construction material as an alternative to Portland cement. Geopolymers can be synthesized using a variety of clay materials, such as fly ash and metakaolin (Rhu *et al*., 2013; Duan *et al*., 2015). In recent years, geopolymers have been investigated intensively as a green environment-friendly material. Geopolymers exhibit good durability, thermal stability, and acid resistance (Duxson *et al*., 2007; Guo and Shi, 2012). Because of these characteristics, geopolymers are widely used for construction materials (Khalifeh *et al*., 2014; Sarker *et al*., 2014; Perná *et al*., 2015), water treatment (Zhang and Liu, 2013), the disposal of solid waste (Pereira *et al*., 2009), and the adsorption of heavy metals (An *et al*., 2008).

As a consequence, several research efforts have been applied to transform geopolymers into zeolites due to the zeolite-like structure of geopolymers. Zeolite structures are composed of TO_4 tetrahedra connected together in three-dimensional space by sharing common oxygen atoms (where T may be Al, Si, or P) (Diaz and Mayoral, 2011). In the traditional synthesis methods, the gel from sources of silica and alumina under alkaline conditions are transformed into zeolites by using templates through a hydrothermal process (Cao *et al*., 1996; Shafiei *et al*., 2014; Narayanan *et al*., 2015). Hence, a novel way to transform geopolymers into zeolites has been investigated recently. Provis *et al.* (2005) speculated about the potential existence of a zeolite-like nano-crystalline structure in geopolymers and that the structure of geopolymers was similar to zeolite precursor materials. Later, Provis and van Deventer (2007) proved that geopolymers could be transformed into zeolites if some requirements were met. Cui *et al.* (2011) and He *et al.* (2013) synthesized NaA zeolites from an Al_2O_3-$2SiO_2$-Na_2O-$7H_2O$ geopolymer through a hydrothermal reaction. Zhang *et al.* (2014) synthesized self-supporting faujasite zeolite membranes from a metakaolin-based geopolymer by *in situ* hydrothermal treatment at 90ºC for 15 h. Liu *et al.* (2016) successfully synthesized a faujasite block at 70ºC in 24 h from a fly ash-based geopolymer *via* a hydrothermal method. These findings suggested that geopolymers could be transformed into zeolites under the appropriate hydrothermal conditions.

The controlled preparation of geopolymers and transformation into zeolites, however, is one of the most challenging tasks in zeolite research due to the complex composition of the materials, which greatly limits the applications of geopolymers transformed into zeolite. Among the several types of zeolite (faujasite (FAU), gismondine (GIS), and mordenite (MOR)),

* E-mail address of corresponding author:
chenjieyu@cug.edu.cn
DOI: 10.1346/CCMN.2016.064048

Table 1. XRF chemical composition (wt.%) of metakaolin heated at 800ºC.

SiO_2	Al_2O_3	Fe_2O_3	TiO_2	CaO	MnO	Na_2O	K_2O	P_2O_5	LOI
52.01	42.76	0.66	0.34	0.056	0.01	0.28	0.41	0.44	3.08

LOI: Loss on ignition at 1000ºC

zeolite P1 is relatively stable for the gismondine-like framework and has a two-dimensional pore system with two intersecting 8-membered oxygen ring channels of 0.31 nm × 0.44 nm and 0.26 nm × 0.49 nm in the [100] and [010] directions, respectively (Breck, 1974). Zeolite P1 has attracted great interest for use in the separation of liquid and gas molecules, the removal of radioactive and toxic waste species, and the adsorption of heavy metals from wastewaters due to the special pore size (Huo *et al.*, 2012).

In this work, research on the preparation of zeolite P1 from a metakaolin-based geopolymer is presented. The goal of the study was to synthesize zeolite P1 by adjusting the hydrothermal conditions. Furthermore, the importance of the N_2 adsorption capacity (*i.e.* specific surface area) is well established for applications of zeolite P1. Notably, this synthesis method was aimed to provide a controllable way to synthesize zeolite P1 and extend the applications of geopolymers.

MATERIALS AND METHODS

Materials

A kaolinite sample was collected from the coal series kaolin of Datong in Shanxi Province, China. The kaolinite was calcined at 600ºC for 4 h to yield a metakaolin product with a high pozzolanic activity, which was used as the raw material to prepare a geopolymer. The chemical composition of the metakaolin is listed in Table 1. The sodium silicate solution was obtained from the Foshan Zhongfa sodium silicate factory, China. The sodium silicate solution had a modulus of 2.8. The sodium hydroxide (NaOH) was a reagent-grade chemical obtained from Sinopharm Chemical Reagent Co, Ltd, China and deionized water was used in all experiments.

Zeolite P1 Synthesis

The process to prepare zeolite P1 is shown in Figure 1. Firstly, an alkali-activated solution (SiO_2/Na_2O molar ratio of 1.0) was prepared by dissolving 10 g of NaOH in 50 mL of sodium silicate solution. Then, 60 g of metakaolin was added into the alkali activated solution and stirred for 20 min until the homogeneous colloid was formed, where the mass ratio of metakaolin, sodium silicate solution, and NaOH were set to be 6:5:1. The slurry was cast into a stainless-steel cube mold (20 mm × 20 mm × 20 mm) and shaken for 2 min to eliminate air bubbles. Next, the sample in the mold was cured at 90ºC at 100% relative humidity for 30 min to accelerate the hardening. After that, the cube-shaped sample was taken out of the mold, sealed with polyethylene (PE) film, and cured at 60ºC in a water bath for 2 h. After curing, the metakaolin-based geopolymer product was denoted MK-GEO.

The MK-GEO samples were placed into 100-mL Teflon bottles that contained different concentrations of NaOH solution and were maintained at 80−120ºC for 5−36 h. Next, the hydrothermally treated samples were separated from the solution and washed thoroughly in deionized water several times until the pH was <10. Afterwards, the samples were dried at 105ºC for 2 h to produce the final hydrothermal products.

Characterization

The chemical composition of the metakaolin was measured using a PANalytical AXIOS^{mAX} X-Ray fluorescence (XRF) instrument (PANalytical, Amelo, The Netherlands). The mineral phases in the samples

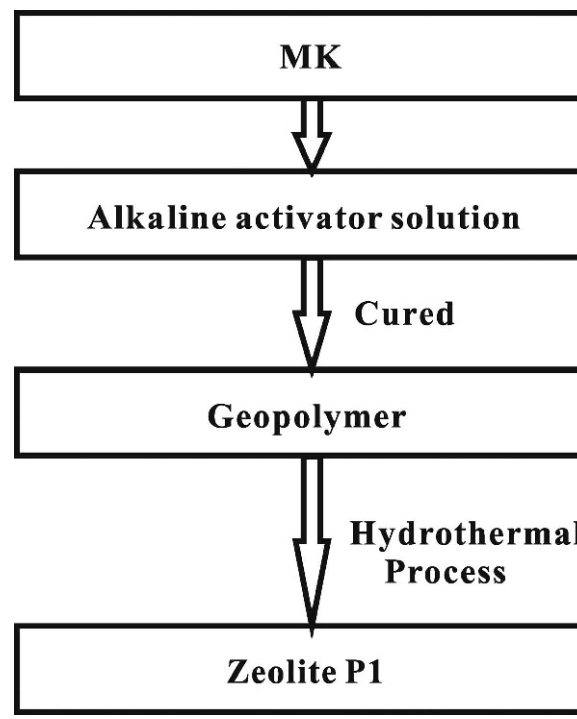

Figure 1. The process used to prepare zeolite P1.

https://doi.org/10.1346/CCMN.2016.064048 Published online by Cambridge University Press

were identified using a Bruker AXS D8-FOCUS X-ray powder diffractometer (XRD) (Bruker AXS, Karlsruhe, Germany) and were step-scanned from 5º to 70º2θ at 4º/min using CuKα radiation, a Ni filter, 40 kV, and 40 mA. The morphology of the samples was characterized using a Hitachi SU8010 field emission scanning electron microscope (FE-SEM) (Hitachi, Tokyo, Japan) operated at an accelerating voltage of 10 kV. Nitrogen gas adsorption/desorption experiments were performed at 77 K using a Micromeritics ASAP2020 automatic surface area and porosimetry system (Micromeritics, Norcross, Georgia, USA) and the specific surface areas were calculated using the Brunauer-Emmett-Teller (BET) method (Brunauer *et al*., 1938).

RESULTS AND DISCUSSION

Hydrothermal Product Crystalline Phase and Morphology

X-ray diffraction. The XRD patterns of the MK-GEO (SiO_2:Al_2O_3 = 3.2), the hydrothermal product, and the standard zeolite P1 (JCPDS cards No. 39-0219) are shown in Figure 2. No evident diffraction peaks were observed in the MK-GEO XRD pattern (Figure 2a), which suggests an X-ray amorphous structure. The XRD pattern of the zeolite P1 (Figure 2b) prepared by hydrothermal treatment using 2.0 mol/L NaOH solution at 100ºC for 24 h had the typical diffraction peaks observed for the standard zeolite P1 (Figure 2c), which demonstrates that the hydrothermal product was zeolite P1. The prepared zeolite P1 XRD pattern (Figure 2b) revealed a single phase material with a high phase purity. These XRD patterns confirmed that zeolite P1 could be synthesized from MK-GEO under controlled conditions.

The lattice parameters of the hydrothermal product were determined using the Rietveld method and XRD data and the final R-values were Rp = 7.67%, Rwp = 9.77%, and Rexp = 2.57%. In comparison to the lattice parameters of the standard zeolite P1 sample (Table 2), the lattice parameters of the hydrothermal product (zeolite P1) were slightly lower and indicated a typical tetragonal system ($a = b < c$) structure.

Scanning electron microscopy. The SEM images (Figure 3) show the particle morphologies of the MK-GEO (SiO_2:Al_2O_3 = 3.2) sample and the hydrothermal product (zeolite P1). The MK-GEO sample micrograph had no evident zeolite structure and apparently still contained an undissolved metakaolin layer (Figure 3a). The hydrothermal product had the typical zeolite P1 morphology with spherical particles (Cardoso *et al*., 2015; Qiu *et al*., 2015) and the particles were around 14.5 μm in diameter (Figure 3b). The evidence of a regular and orderly morphology in the micrograph suggests a well crystallized zeolite P1 sample and further confirmed that zeolite P1 was successfully prepared from MK-GEO through the hydrothermal process.

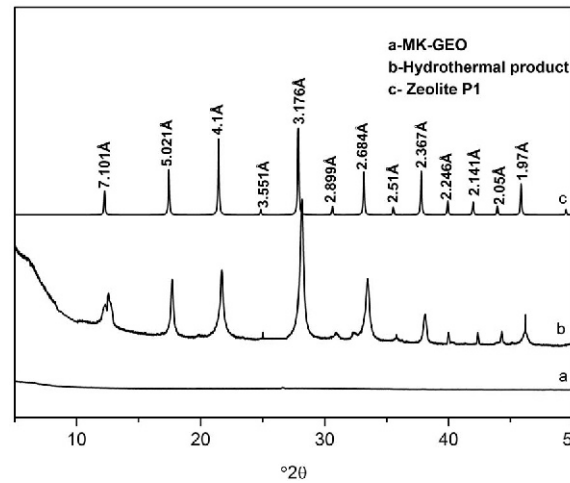

Figure 2. XRD patterns of (a) MK-GEO, (b) hydrothermal synthesis product, and (c) a standard zeolite P1 sample.

N_2 adsorption isotherms. Nitrogen sorption/desorption isotherms at 77 K for the zeolite P1 prepared from MK-GEO (Figure 4) revealed a typical type IV isotherm (defined by International Union of Pure and Applied Chemistry (IUPAC)) with a small hysteresis loop in the desorption branch at high relative pressures, which implies a typical meso-macroporous material with a large interparticle porosity. The hysteresis loop, which looked somewhat like an inverse type H3 hysteresis, may be attributed to the occurrence of pore blocking and a wide distribution of independent pores. Inverse type H3 hysteresis has been observed for samples with large adsorption capacities at high relative pressures, which is considered to be due to assemblages of slit-shaped pores by the association of kaolinite platelets (Thommes, 2010). The microstructure parameters of zeolite P1 were summarized as follows: the BET specific

Table 2. Crystal structure parameters of the hydrothermal product and the standard zeolite P1 sample.

Sample	*a*	*b*	*c*	α	β	γ
Hydrothermal product	10.01 Å	10.01 Å	10.03 Å	90º	90º	90º
Standard zeolite P1	10.04 Å	10.04 Å	10.04 Å	90º	90º	90º

https://doi.org/10.1346/CCMN.2016.064048 Published online by Cambridge University Press

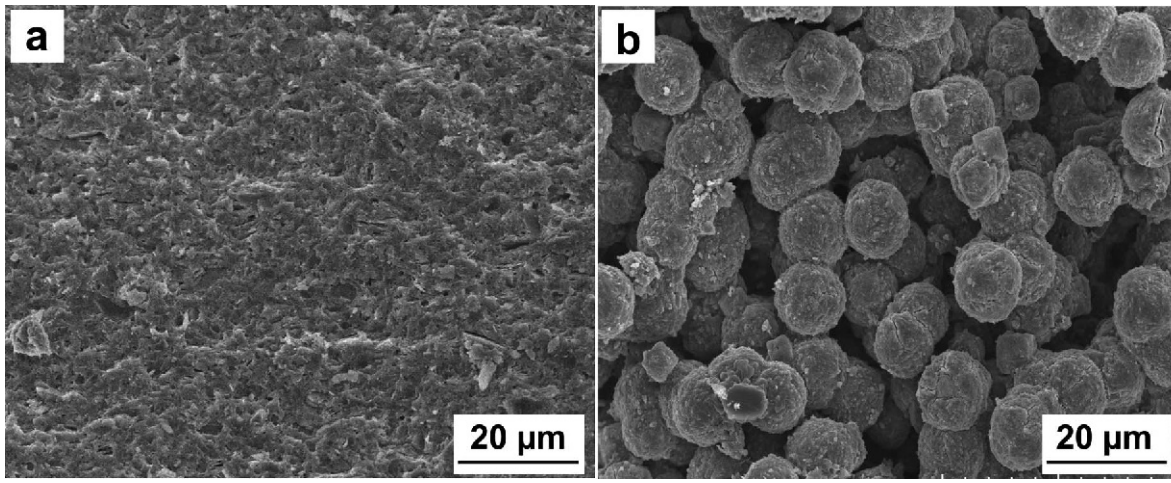

Figure 3. The morphology of (a) MK-GEO and (b) hydrothermal synthesis product.

surface area was 36.56 m^2/g, the total pore volume was 0.097 cm^3/g and the average diameter of mesopores was 13.26 nm. The BET surface area of the synthesized zeolite P1 was lower than published values (46.5 m^2/g). The lower surface area might be explained by pore blocking due to the association of kaolinite platelets and residual SiO_2 and Al_2O_3 in the MK that did not fully react (Ma *et al*., 1998; Sharma *et al*., 2016).

Effects of reaction conditions

Hydrothermal temperature. In this group of experiments, the hydrothermal products were prepared from MK-GEO (SiO_2:Al_2O_3 = 3.2) in 2.0 mol/L NaOH solution at 80ºC, 90ºC, 100ºC, 110ºC, and 120ºC for 24 h. According to the XRD patterns of the hydrothermal products (Figure 5), MK-GEO was transformed into the zeolites faujasite (FAU), zeolite P1, sodalite (SOD), and analcite, respectively, as the hydrothermal temperature was increased from 80ºC to 120ºC. As shown in Figure 5, the lower 110ºC temperature produced FAU, while the higher 120ºC temperature tended to produce SOD and analcite. The hydrothermal temperature to produce zeolite P1 was, hence, between 110ºC and 120ºC, which is consistent with published reports (Valtchev and Bozhilov, 2004; Mao *et al*., 2013; Zhang *et al*., 2014; Liu *et al*., 2016). The XRD patterns in Figure 5 indicate that zeolite P1 was produced at 90ºC to ~120ºC and pure zeolite P1 was observed at 100ºC. Below and above the 90ºC to ~120ºC temperature range, FAU was formed in addition to the other zeolite phases. From published reports, FAU zeolites can develop from the same composition (Na_2O, Al_2O_3, SiO_2, and H_2O) and thus compete with zeolite NaP (Breck, 1974; Chandrasekhar and Pramada, 1999). As the hydrothermal reaction temperature was increased from 100ºC to 120ºC, the intensity of zeolite P1 diffraction peaks decreased and was accompanied by a mixture of FAU, SOD, and analcite. The SOD and analcite are believed to form secondary building units at high temperatures, which generally leads to a higher degree of zeolite formation (Park *et al*., 2000; Qiu *et al*., 2015).

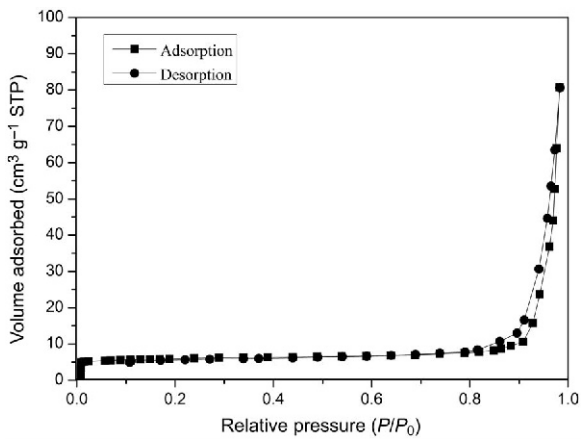

Figure 4. N_2 adsorption-desorption isotherms of zeolite P1.

The SEM images of the samples prepared at different temperatures (Figure 6) show that the morphologies clearly changed as the hydrothermal temperature was increased from 80ºC to 120ºC. A few clusters of FAU conjoined together with irregular shapes appeared on the surface of MK-GEO at 80ºC, but the material was mostly amorphous (Figure 6a). When the temperature was increased to 90ºC, FAU crystals with octahedral shapes almost fill up the field of view in the micrograph (Figure 6b) and the size of the crystals was 2–~3 μm and included a small amount of zeolite P1. The particles of the sample synthesized at 100ºC exhibited a high degree of crystallinity, had a ball-like shape, and a uniform size of 14.5 μm. When the temperature was increased to 110ºC (Figure 6d), the surface of zeolite P1 particles with a ball-like shape became rough and

https://doi.org/10.1346/CCMN.2016.064048 Published online by Cambridge University Press

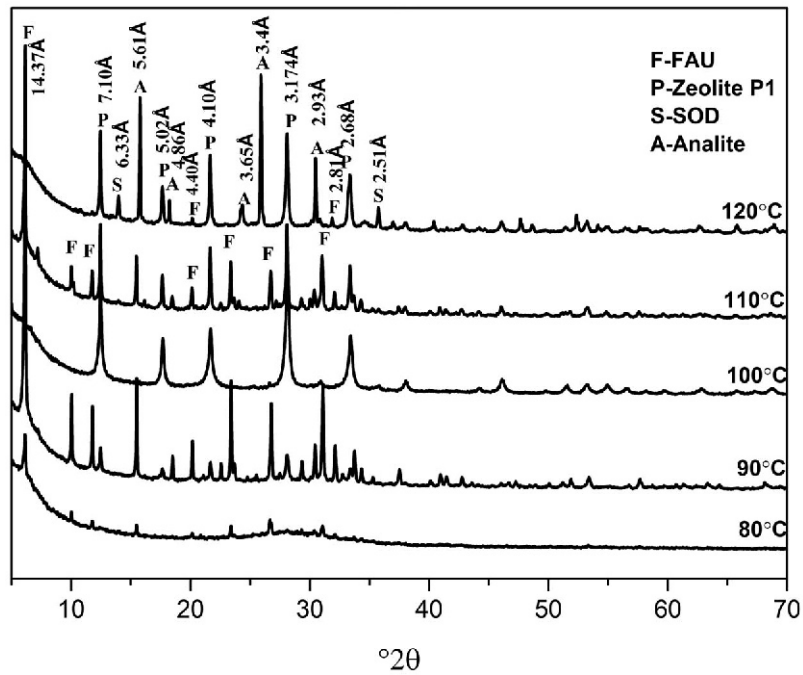

Figure 5. XRD patterns of hydrothermal products synthesized at 80, 90, 100, 110, and 120ºC.

irregular. This demonstrates that zeolite P1 was beginning to dissolve under the highly alkaline conditions, while FAU crystals started to appear. As the temperature was increased to 120ºC (Figure 6e), the wool-ball-like shape of SOD and a conglomeration of analcite particles with sharp edges appeared together around zeolite P1 (Murayama *et al*., 2002; Qiu *et al*., 2015) and this SEM observation was also in great agreement with the XRD

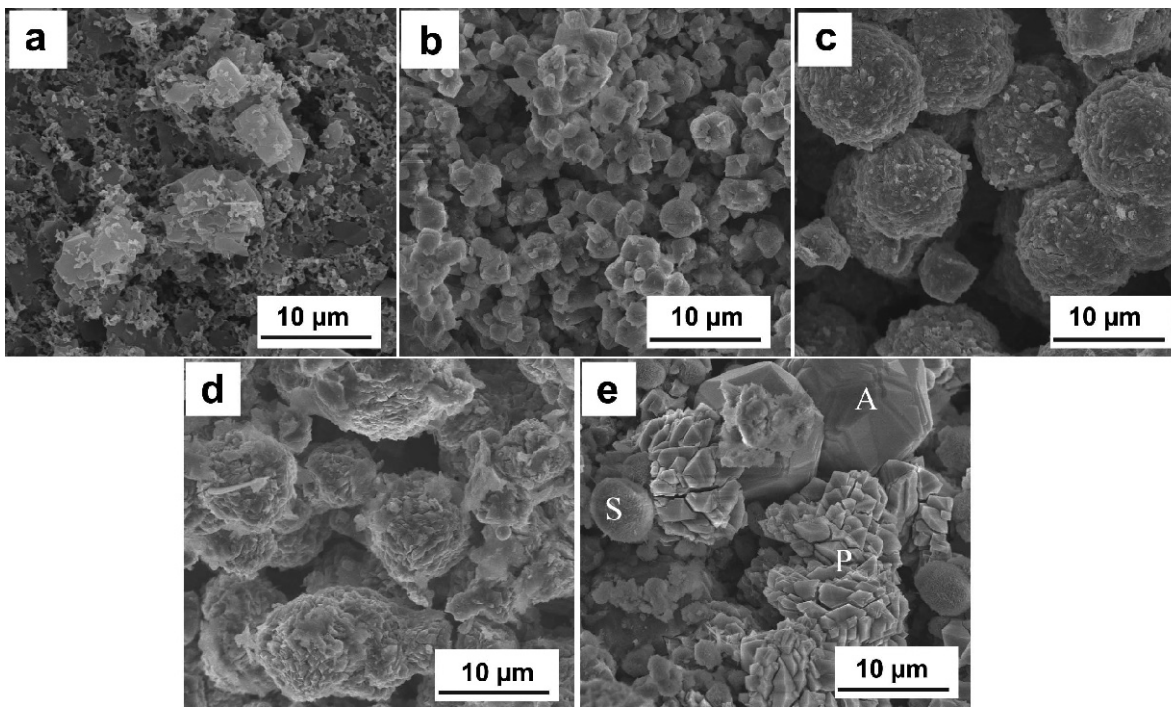

Figure 6. SEM images of the hydrothermal products prepared at (a) 80, (b) 90, (c) 100, (d) 110, and (e) 120ºC.

https://doi.org/10.1346/CCMN.2016.064048 Published online by Cambridge University Press

patterns. After considering the crystallinity and the morphology of the hydrothermal products at 100ºC, the hydrothermal process to prepare zeolite P1 was finally determined.

Hydrothermal solution alkalinity. In order to determine the effects of alkalinity on the properties of the resultant products, the hydrothermal products were prepared from MK-GEO in 1.0 mol/L to 2.5 mol/L NaOH solution at 100ºC for 24 h. As can be seen in the XRD pattern (Figure 7), the hydrothermal product formed at $\leqslant$1.5 mol/L NaOH has no obvious diffraction peaks. This indicates that the geopolymer cannot be transformed into zeolites under the lower alkalinity conditions due to little or no crystallization (Murayama *et al*., 2002). As NaOH solution concentrations were increased from 1.8 mol/L to 2.0 mol/L, the XRD peaks of zeolite P1 gradually increased in intensity. The condensation of silica and aluminate ions in the geopolymer could be enhanced by adding a small amount of OH^- (Murayama *et al*., 2002). When the alkalinity was higher than 2 mol/L NaOH, a mixture of zeolite P1, FAU, and SOD appeared, which revealed that the hydrothermal conversion of MK-GEO to zeolite at higher alkalinities results in the conversion of zeolite P1 to a more stable SOD phase (Park *et al*., 2000; Aldahri *et al*., 2016). The 1.8 mol/L to ~2.0 mol/L NaOH solutions were, therefore, more suitable for the preparation of zeolite P1.

The SEM micrographs indicated changes in the morphology (Figure 8). The structures in the samples (Figure 8a and 8b) appeared to be mostly amorphous when the alkalinity was 1.0 mol/L to ~1.5 mol/L NaOH. The initial morphology of the geopolymer was maintained without zeolite formation and was coupled with a small amount of undissolved metakaolin layers (Figure 8a), which was expected because the zeolite nuclei were covered by an amorphous gel (Valtchev and Bozhilov, 2004). When the alkalinity was increased to 1.8 mol/L NaOH (Figure 8c), spherical-shaped zeolite P1 particles were formed. In comparison to the sample synthesized at an alkalinity of 1.8 mol/L NaOH, however, the sample synthesized at 2.0 mol/L NaOH had perfect crystals with sharp edges and a homogeneous particle size of 14.5 μm (Figure 8d). By further increasing the alkalinity to 2.5 mol/L NaOH (Figure 8e), the size of the spherical zeolite particles decreased and FAU particles with an octahedral shape and wool-ball like SOD particles were formed simultaneously. This means that zeolite P1 was dissolved under the higher alkalinity, which, in contrast, contributed to the growth of FAU and SOD. Accordingly, the XRD and SEM results indicate that a 2.0 mol/L NaOH concentration was the optimal alkalinity to convert MK-GEO into zeolite P1.

Hydrothermal reaction time. To determine the effects of hydrothermal reaction time on the properties of the resultant products, the hydrothermal products were prepared from MK-GEO at 100ºC for 5 h to ~36 h in 2.0 mol/L NaOH solution. According to the XRD pattern

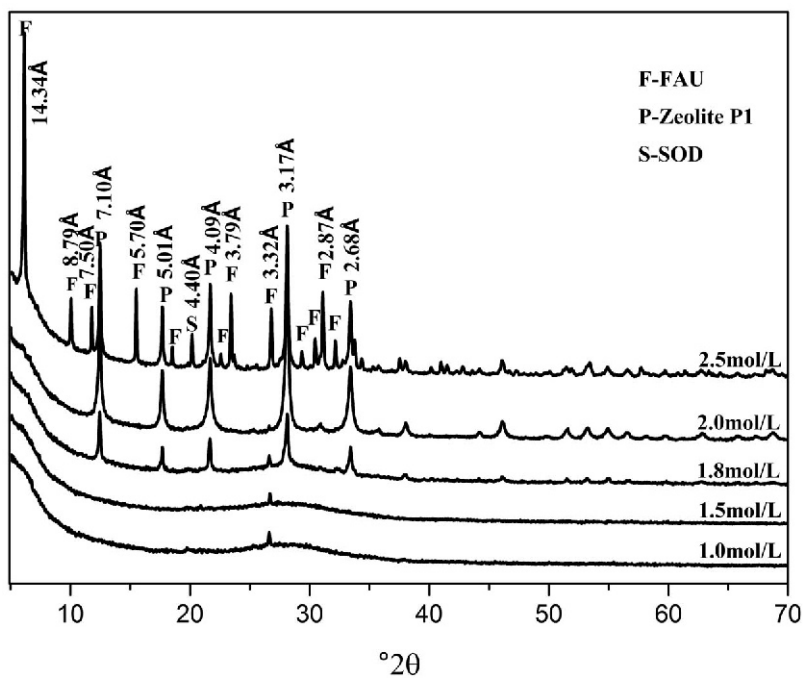

Figure 7. XRD patterns of the hydrothermal products synthesized at alkalinites of 1.0, 1.5, 1.8, 2.0, and 2.5 mol/L NaOH.

https://doi.org/10.1346/CCMN.2016.064048 Published online by Cambridge University Press

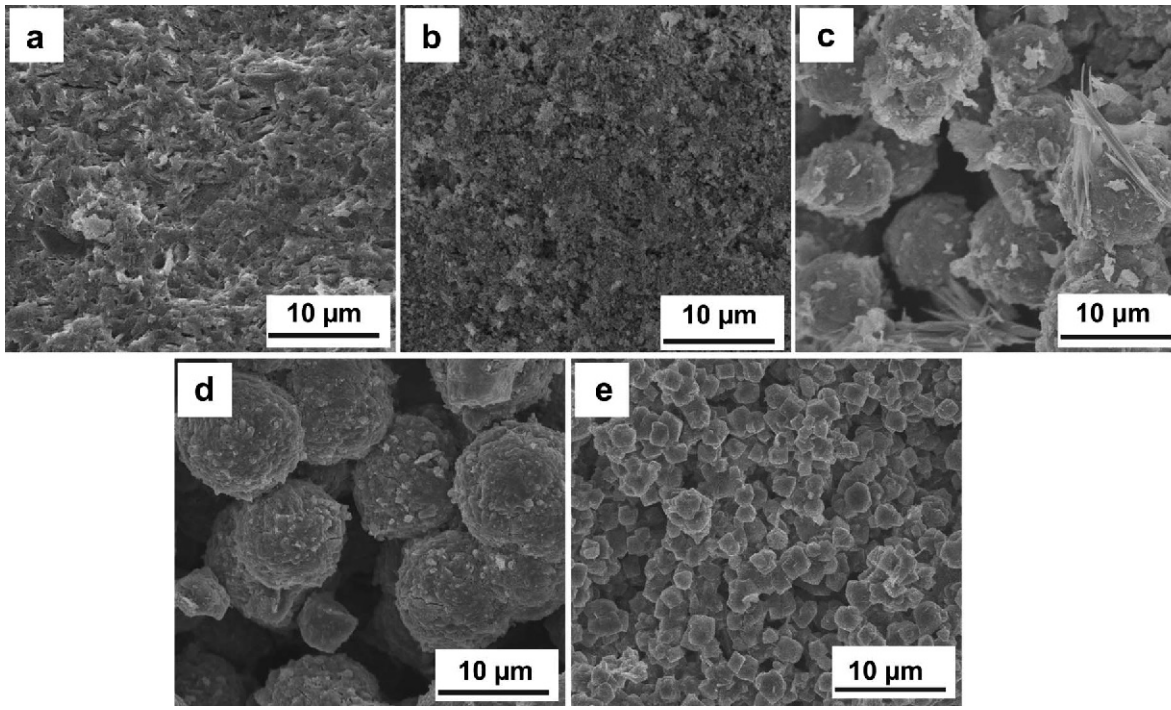

Figure 8. SEM images of the hydrothermal products synthesized at alkalinities of (a) 1.0, (b) 1.5, (c) 1.8, (d) 2.0, and (e) 2.5 mol/L NaOH.

(Figure 9), an amorphous phase was mostly observed after a reaction time of 5 h, which indicated that MK-GEO did not transform into zeolite under the short reaction time (Askari *et al*., 2013). With an extension in the hydrothermal reaction time from 12 h to 18 h, the final products were FAU crystals with a greater crystallinity. A 12 h to ~18 h hydrothermal reaction time, hence, was suitable for the growth of FAU. The pure

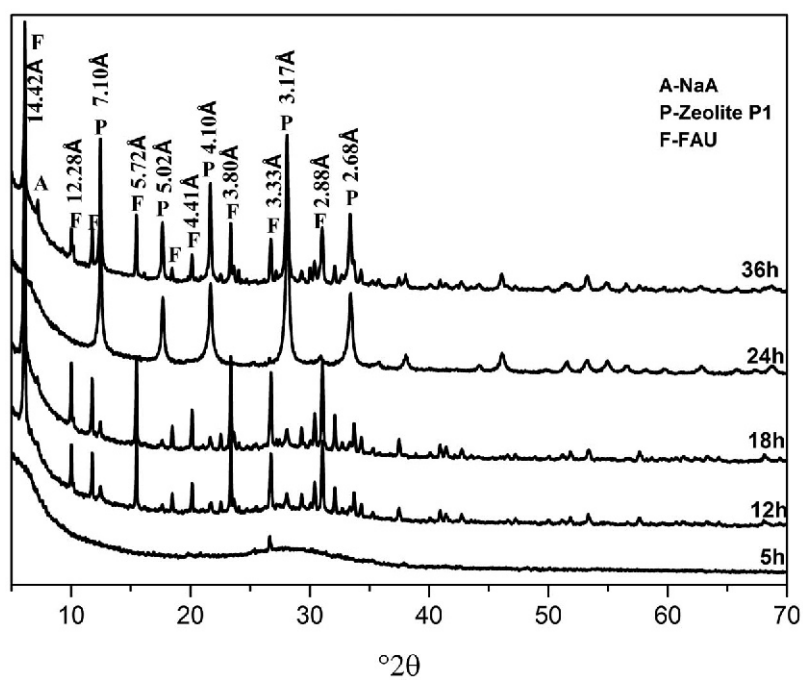

Figure 9. XRD patterns of products synthesized at hydrothermal reaction times of 5, 12, 18, 24, and 36 h.

https://doi.org/10.1346/CCMN.2016.064048 Published online by Cambridge University Press

zeolite P1 was observed when the hydrothermal reaction time was 24 h. Further increasing the hydrothermal reaction time to 36 h, however, produced a mixture of zeolite P1, FAU, and NaA, which indicated that a long hydrothermal reaction time provided enough activation energy to collapse the structure and to increase soluble Si and Al species concentrations needed for the re-crystallization and growth of FAU and NaA phases (Askari *et al*., 2013).

The micrograph of the final products synthesized at different hydrothermal reaction times reflected the microscopic changes (Figure 10). Synthesized products with an amorphous structure were evident at hydrothermal reaction times of 5 h (Figure 10a). When the hydrothermal reaction time was increased from 12 h to 18 h, typical FAU crystals were formed and are shown in Figures 10b and 10c, respectively. At a hydrothermal reaction time of 24 h, spherically shaped zeolite P1 crystals were identified (Figure 10d). When the hydrothermal reaction time was increased to 36 h, the surfaces of zeolite P1 were roughened due to long exposure to high alkali concentrations, the particles were larger and with more irregular shapes (Figure 10e). The product was assigned to the formation of FAU and NaA zeolites (Valtchev and Bozhilov, 2004; Hu *et al*., 2008; Liu *et al*., 2013; Bohra *et al*., 2014). Nevertheless, a 24 h hydrothermal reaction time was suitable for the synthesis of pure zeolite P1.

Reaction mechanism

The reaction mechanism for the transformation of MK-GEO into zeolite P1 was investigated. First, the dissolution reaction of the raw materials as silicate and aluminate sources occurred in the presence of OH^- (equation 1). Next, the condensation of silicate ions ($[SiO_2(OH)]^{2-}$) and aluminate ions ($[Al(OH)_4]^-$) began to take place in order to form an aluminosilicate gel (equation 2) (Khale and Chaudhary, 2007). As the condensation reaction proceeded, the amorphous structure of MK-GEO was formed by the irregular arrangement of $[SiO_4]$ and $[AlO_4]$ tetrahedral frameworks in three dimensions. The MK-GEO could transform into zeolite from secondary zeolite building units that existed in the geopolymer. Then, zeolite crystallization occurred under the appropriate hydrothermal conditions, where the $[SiO_4]$ and $[AlO_4]$ tetrahedral frameworks were rearranged by adjustment of the bond angles. Finally, the eight-membered ring of the gismondine-like structure of zeolite P1 was formed (Murayama *et al*., 2002).

$$(SiO_2,Al_2O_3)_n + 3OH^- + 3H_2O \rightarrow 2n[Al(OH)_4]^- + n[SiO_2(OH)_2]^{2-} \quad (1)$$

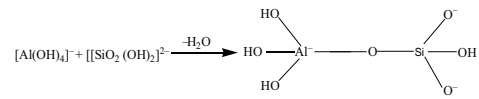

(2)

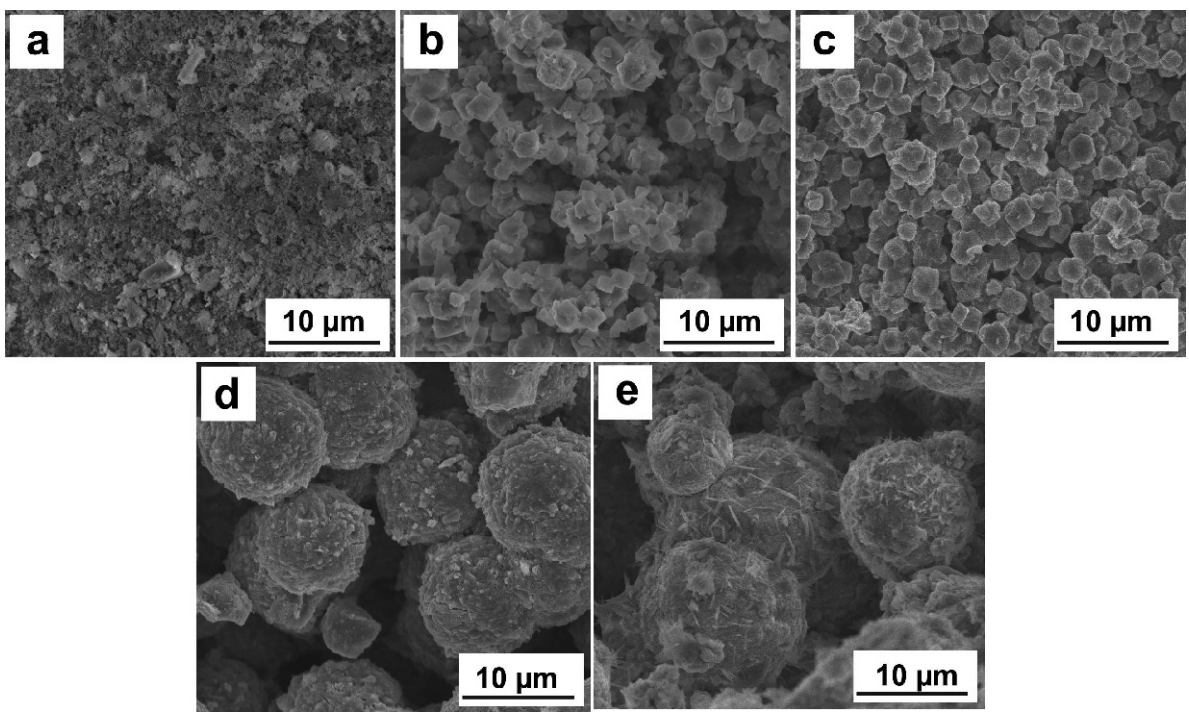

Figure 10. SEM images of hydrothermal products synthesized at hydrothermal reaction times of (a) 5, (b) 12, (c) 18, (d) 24, and (e) 36 h.

https://doi.org/10.1346/CCMN.2016.064048 Published online by Cambridge University Press

CONCLUSIONS

In summary, zeolite P1 was synthesized via a hydrothermal reaction from a metakaolin-based geopolymer. The synthesized zeolite P1 had a spherical shape, a uniform size, and high crystallinity at the optimal hydrothermal conditions of 100ºC for 24 h in 2.0 mol/L NaOH solution. The structure and morphology of the synthesized zeolite can be controlled by adjusting the hydrothermal temperature, alkalinity, and reaction time. Furthermore, the synthesized zeolite P1 had a BET specific surface area of 36.56 cm^3g^{-1}. Compared with the conventional synthesis route used to prepare zeolites, this method can be widely used in synthesizing zeolites by adjustment of the preparation parameters and the added value of a clay mineral material-based geopolymer was expanded.

ACKNOWLEDGMENTS

The project was supported by the Fundamental Research Funds for the Central Universities, China University of Geosciences (Wuhan) (CUG160231), and the National Natural Science Foundation of China (51502272).

REFERENCES

Aldahri, T., Behin, J., Kaezemin, H., and Rohani, S. (2016) Synthesis of zeolite Na-P from coal fly ash by thermo-sonochemical treatment. *Fuel*, **182**, 494–501.

An, J.P., Lu, Z.Y., and Yan, Y. (2008) Status and outlook of study on immobilization of heavy metal and radioactive waste with fly ash based geopolymer. *Atomic Energy Science and Technology*, Issue 12, 1086–1091.

Askari, S., Miar Alipour, S., Halladj, R., and Davood Abadi Farahani, M.H. (2013) Effects of ultrasound on the synthesis of zeolites: a review. *Journal of Porous Materials*, **20**, 285–302.

Bohra, S., Kundu, D., and Naskar, M.K. (2014) One-pot synthesis of NaA and NaP zeolite powders using agro-waste material and other low cost organic-free precursors. *Ceramics International*, **40**, 1229–1234.

Breck, D.W. (1974) *Zeolite Molecular Sieves: Structure, Chemistry, and Use*. Wiley, New York.

Brunauer, S., Emmett, P.H., and Teller, E. (1938) Adsorption of gases in multimolecular layers. *Journal of the American Chemical Society*, **60**, 309–319.

Cao, G., Lu, Y., Delattre, L., Brinker, C.J., and López, G.P. (1996) Amorphous silica molecular sieving membranes by sol-gel processing. *Advanced Materials*, **8**, 588–591.

Cardoso, A.M., Paprocki, A., Ferret, L.S., Azevedo, C.M., and Pires, M. (2015) Synthesis of zeolite Na-P1 under mild conditions using Brazilian coal fly ash and its application in wastewater treatment. *Fuel*, **139**, 59–67.

Chandrasekhar, S. and Pramada, P.N. (1999) Investigation on the synthesis of zeolite NaX from Kerala kaolin. *Journal of Porous Materials*, **6**, 283–297.

Cui, X., He, Y., Liu, L., and Chen, J. (2011) NaA zeolite synthesis from geopolmer precursor. *MRS Communications*, **1**, 49–51.

Davidovits, J. (1991) Geopolymers. *Journal of Thermal Analysis*, **37**, 1633–1656.

Diaz, I., and Mayoral, A. (2011) TEM studies of zeolites and ordered mesoporous materials. *Micron*, **42**, 512–527.

Duan, P., Yan, C., Zhou, W., Luo, W., and Shen, C. (2015) An investigation of the microstructure and durability of a fluidized bed fly ash-metakaolin geopolymer after heat and acid exposure. *Materials & Design*, **74**, 125–137.

Duxson, P., Fernández Jiménez, A., Provis, J.L., Lukey, G.C., Palomo, A., and van Deventer, J.S.J. (2007) Geopolymer technology: The current state of the art. *Journal of Materials Science*, **42**, 2917–2933.

Guo, X.L. and Shi, H.S. (2012) Self-solidification/stabilization of heavy metal wastes of class C fly ash-based geopolymers. *Journal of Materials in Civil Engineering*, **25**, 491–496.

He, Y., Cui, X.M., Liu, X.D., Wang, Y.P., Zhang, J., and Liu, K. (2013) Preparation of self-supporting NaA zeolite membranes using geopolymers. *Journal of Membrane Science*, **447**, 66–72.

Hu, D., Xia, Q.H., Lu, X.H., Luo, X.B., and Liu, Z.M. (2008) Synthesis of ultrafine zeolites by dry-gel conversion without any organic additive. *Materials Research Bulletin*, **43**, 3553–3561.

Huo, Z., Xu, X., Lü, Z., Song, J., He, M., Li, Z., Wang, Q., and Yan, L. (2012) Synthesis of zeolite NaP with controllable morphologies. *Microporous and Mesoporous Materials*, **158**, 137–140.

Khale, D. and Chaudhary, R. (2007) Mechanism of geopolymerization and factors influencing its development: a review. *Journal of Materials Science*, **42**, 729–746.

Khalifeh, M., Saasen, A., Vralstad, T., and Hodne, H. (2014) Potential utilization of class C fly ash-based geopolymer in oil well cementing operations. *Cement and Concrete Composites*, **53**, 10–17.

Liu, X.D., Wang, Y.P., Cui, X.M., He, Y., and Mao, J. (2013) Influence of synthesis parameters on NaA zeolite crystals. *Powder Technology*, **243**, 184–193.

Liu, Y., Yan, C., Qiu, X., Li, D., Wang, H., and Alshameri, A. (2016) Preparation of faujasite block from fly ash-based geopolymer via *in situ* hydrothermal method. *Journal of the Taiwan Institute of Chemical Engineers*, **59**, 433–439.

Ma, W., Brown, P.W., and Komarneni, S. (1998) Characterization and cation exchange properties of zeolite synthesized from fly ashes. *Journal of Materials Research*, **13**, 3–7.

Mao, J., Wang, Y., Liu, J., He, Y., Liu, X., and Cui, X. (2013) *In situ* synthesis of faujasite zeolite membrane from geopolymer and its pervaporation properties. *Journal of the Chinese Ceramic Society*, **41**, 1244–1250.

Murayama, N., Yamamoto, H., and Shibata, J. (2002) Mechanism of zeolite synthesis from coal fly ash by alkali hydrothermal reaction. *International Journal of Mineral Processing*, **64**, 1–17.

Narayanan, S., Vijaya, J.J., Sivasanker, S., Kennedy, L.J., and Jesudoss, S. (2015) Structural, morphological and catalytic investigations on hierarchical ZSM-5 zeolite hexagonal cubes by surfactant assisted hydrothermal method. *Powder Technology*, **274**, 338–348.

Park, M., Choi, C.L., Lim, W.T., Kim, M.C., Choi, J., and Heo, N.H. (2000) Molten-salt method for the synthesis of zeolitic materials: II. Characterization of zeolitic materials. *Microporous and Mesoporous Materials*, **37**, 91–98.

Pereira, C.F., Luna, Y. and Querol, X. (2009) Waste stabilization/solidification on an electric arc furnace dust using fly ash-based geopolymers. *Fuel*, **88**, 1185–1193.

Perná, I., Hanzlíček, T., Boura, P., and Lučaník, A. (2016) The manufacture of grinding wheels based on the Ca-K geopolymer matrix. *Materials and Manufacturing Processes*, **31**, 667–672.

Provis, J.L. and van Deventer, J.S.J. (2007) Geopolymerisation kinetics. 2. Reaction kinetic modelling. *Chemical Engineering Science*, **62**, 2318–2329.

Provis, J.L. and van Deventer, J.S.L. (2009) Introduction to

geopolymers. Pp 1–11. In J.L. Provis and J.S.L. van Deventer (eds.) *Geopolymers: Stuctures, Processing, Properties and Industrial Applications*. Woodhead Publishing Limited, CRC Press, New York, NY.

Provis, J.L., Lukey, G.C., and van Deventer, J.S.J. (2005) Do geopolymers actually contain nanocrystalline zeolites? A reexamination of existing results. *Chemistry of Materials*, **17**, 3075–3085.

Qiu, X.M., Liu, Y.D., Li, D., and Yan, C.J. (2015) Preparation of NaP zeolite block from fly ash-based geopolymer via in situ hydrothermal method. *Journal of Porous Materials*, **22**, 291–299.

Ryu, G.S., Lee, Y.B., Koh, K.T., and Chung, Y.S. (2013) The mechanical properties of fly ash-based geopolymer concrete with alkaline activators. *Construction and Building Materials*, **47**, 409–418.

Sarker, P.K., Kelly, S., and Yao, Z. (2014) Effect of fire exposure on cracking, spalling and residual strength of fly ash geopolymer concrete. *Materials & Design*, **63**, 584–592.

Shafiei, K., Moghaddam, M.K., Pakdehi, S.G., and Mohammadi, T. (2014) Hydrothermal synthesis of nano-sized zeolite T crystals. *Particulate Science and Technology*, **32**, 8–19.

Sharma, P., Song, J.S., Han, M.H., and Cho, C.H. (2016) GIS-NaP1 zeolite microspheres as potential water adsorption material: Influence of initial silica concentration on adsorptive and physical/topological properties. *Scientific Reports*, **6**, 22734.

Thommes, M. (2010) Physical adsorption characterization of nanoporous materials. *Chemie Ingenieur Technik*, **82**, 1059–1073.

Valtchev, V.P. and Bozhilov, K.N. (2004) Transmission electron microscopy study of the formation of FAU-type zeolite at room temperature. *The Journal of Physical Chemistry B*, **108**, 15587–15598.

Zhang, J., He, Y., Wang, Y.P., Mao, J., and Cui, X.M. (2014) Synthesis of a self-supporting faujasite zeolite membrane using geopolymer gel for separation of alcohol/water mixture. *Materials Letters*, **116**, 167–170.

Zhang, Y. and Liu, L. (2013) Fly ash-based geopolymer as a novel photocatalyst for degradation of dye from wastewater. *Particuology*, **11**, 353–358.

(*Received 1 October 2016; revised 24 February 2017; Ms. 1139; AE: S.M. Kuznicki*)